Deformation measurement along two directions of a continuously deforming object by using two lasers and one color camera

doi: 10.1117/12.912076

Deformation measurement along two directions of a continuously deforming object by using two lasers and one color camera

Toshihiro Senzawa and Masaaki Adachi
Division of Mechanical Science and Engineering, Kanazawa University, Kanazawa 920-1192, JAPAN

ABSTRACT

In a previous study, we developed the continuous-deformation measurement method which does not require specklegram in static condition and can measure deformation more than 200 micro-meters with 0.1 micro-meter resolution. This method could be applied to deformation measurement along only one direction. We have improved this method and have obtained the new method which can measure deformation along two directions by using two lasers and one color camera. To verify the validity of the method, we carried out deformation measurement of an aluminum plate which was set at a tension testing machine. Results of deformation measurement along two directions are shown.

1. Introduction

Real-time deformation measurement of a diffuse object can be easily carried out with digital speckle pattern interferometry (DSPI). Because the phase change in the DSPI is quantitatively related to the amount of deformation, many studies have been done to extract accurate phase changes from specklegrams. Among them, phase-shifting[1] is famous technique which can measure accurate deformation of a diffuse object. Phase-sifting technique has been extensively investigated and applied to many practical measurements because of its simplicity and high resolution. However, this technique requires that several specklegrams be captured in the static, non-deforming, condition of an object, making it unsuitable for measuring objects deforming continuously. Another techniques, for example specially designed multicamera,[2] max-min scanning,[3,4] Fourier-transform of carrier fringes,[5] and spatial-carrier phase-shifting techniques,[6] can work well in conditions of continuous deformation. However, they have disadvantageous points. The multicamera system is expensive. The Fourier-transforming[7] and spatial-carrier phase-shifting techniques have considerably less resolution than the phase-shifting technique. In the max-min scanning techniques, two specklegrams are necessary to extract one speckle phase: one was of a deforming object and the other was of a sign image, phase-shifted to the former. Then they were applied to slowly deforming objects. Some techniques that could extract a phase from only one specklegram of a deforming object[8,9] also have been proposed. These techniques require the phase of the specklegram before deformation to extract the phase and need a static condition of the object in order to calculate the required phase through the phase-shifting technique.

Our technique developed in a previous study[9,10] can be used to measure the deformation of objects that have already started a dynamic deformation and that keep deforming. However, this technique could not measure deformation along two directions. We have improved this technique and have obtained the new technique which can measure deformation along two directions by using two lasers and one color camera. Two lasers irradiate an object along different directions to measure deformation along each direction. This paper describes the principle of deformation measurement and shows measurement results.

Photonics, Devices, and Systems V, edited by Pavel Tománek, Dagmar Senderáková, Petr Páta,
Proc. of SPIE Vol. 8306, 83060C · © 2011 SPIE · CCC code: 0277-786X/11/$18 · doi: 10.1117/12.912076

2. Principle of deformation measurement

In subsection 2.1 we describe the extraction technique relating to the speckle phase at the starting point of deformation measurement. Subsection 2.2 concerns the technique to extract the changing phase after the starting point. The technique for extracting the deformation phase in a large object deformation and the technique for measuring deformation along two directions are described in subsection 2.3 and 2.4.

2.1. Speckle Phase at the Starting Point of the Measurement

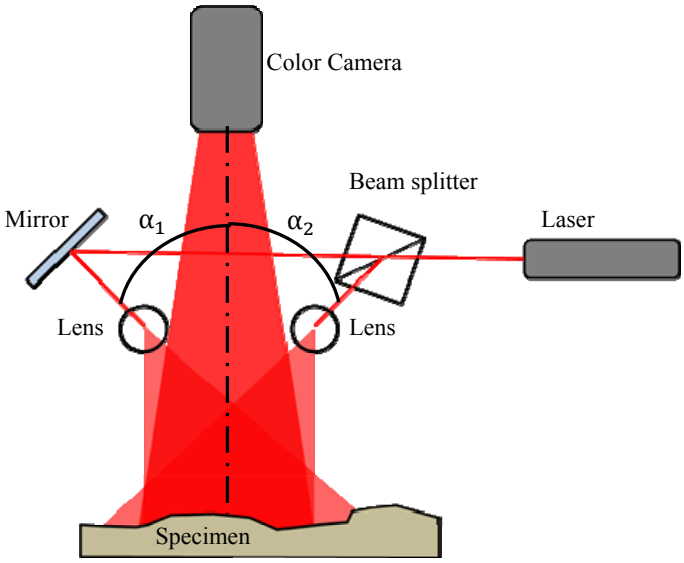

Fig. 1. The optical layout of a DSPI (In this experiment $\boldsymbol{\alpha_1 = \alpha_2 = \alpha}$)

Let us consider the speckle interferometry shown in Fig.1. The interference light intensity $I(\mathbf{r},t)$ at time t and position $\mathbf{r}$ on a diffuse surface is given by

$$I(\mathbf{r},t) = O_D(\boldsymbol{r}) + O_{ALT}(\mathbf{r})\cos\{\theta(\mathbf{r},t)\}. \tag{1}$$

where $O_D(\mathbf{r})$ is the dc component, $O_{ALT}(\mathbf{r})$ is the modulation amplitude, and $\theta(\mathbf{r},t)$ is the phase of the specklegram. When the object is continuously deforming, $I(\mathbf{r},t)$ would take a change shown by the curve in Fig. 2. Recording such an intensity change with a CCD camera can calculate the maximum and the minimum values, $I_{max}(\mathbf{r})$ and $I_{min}(\mathbf{r})$, of the light intensity change on an each pixel. From those values and light intensity $I(\mathbf{r},t_k)$ in specklegram, which is captured at $t = t_k$, the absolute value of the speckle phase $|\theta(\mathbf{r}, t_k)|$ can be calculated by

$$|\theta(\mathbf{r},t_k)| = \cos^{-1}\left\{\frac{I(\mathbf{r},t_k) - \left[\frac{I_{max}(\mathbf{r}) + I_{min}(\mathbf{r})}{2}\right]}{\left[\frac{I_{max}(\mathbf{r}) - I_{min}(\mathbf{r})}{2}\right]}\right\} . \tag{2}$$

We cannot determine a sign, plus or minus, because arccosine is an even function. One of the two values with opposite signs is a right phase and the other is not. Then we consider both signed phase and also consider a deformation phase from t_k to t_l. The following four values δ_{kl} given by

$$\delta_{kl}(\mathbf{r}) = \pm|\theta(\mathbf{r},t_l)| - \{\pm|\theta(\mathbf{r},t_k)|\} . \tag{3}$$

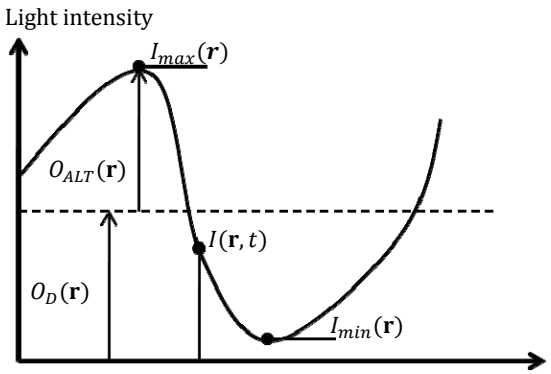

Fig. 2. Light-intensity change on the pixel of a CCD camera due to deformation of the object

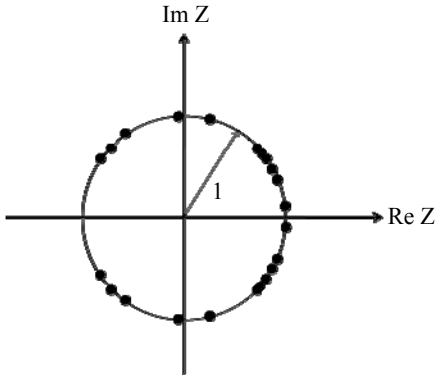

Fig. 3. Complex plane plotting of $\exp[i\delta_{kl}(\boldsymbol{r})]$ in a local area (5 × 5 pixels) where $\delta_{kl}(\boldsymbol{r})$ is given by Eq. (3). The number of points is 100 and some overlap.

are possible solutions for the deformation phase from t_k to t_l. Only one of the four values is right. Such right deformation phases on pixels in a small local area (in this experiment, 5 × 5 pixels) around $\boldsymbol{r}$ should nearly equal one another, because amounts of deformation on pixels in such an area are supposed to be approximately the same. On a complex plane we plot the value of $\exp[i\delta_{kl}(\mathbf{r})]$ in all the pixel position in the small local area. Fig. 3 shows the plotted points. They are distributed symmetrically around the real axis. This symmetry comes from the fact that group values of $\delta_{kl}(\mathbf{r})$ in a small local area are the same as those of $-\delta_{kl}(\mathbf{r})$. Here we restrict our discussion of the distribution to only the upper half of the plane. In those areas 50% of the plotted points are related to the absolute values of the right deformation phases. The other points are affected by random speckle phases that originate from diffuse surface reflection. They are statistically distributed uniformly from 0 to π in phase.

An average value of the points affected by the speckle phase is predicted to be close to $(2/\pi)i$. We therefore average all the plotted values in the upper half of the area and subtract $(2/\pi)i$ from the average values so that we can obtain the absolute value of the deformation phase. Although we have discussed the value of $\exp[i\delta_{kl}(\mathbf{r})]$, we actually average the values of $[I_{max}(\mathbf{r}) - I_{min}(\mathbf{r})]\exp[i\delta_{kl}(\mathbf{r})]$ instead of the values of $\exp[i\delta_{kl}(\mathbf{r})]$ so that low modulation data, which are sensitive to electric noise and digitizing error etc., can have less influence and high modulation data can have more influence on the average value. Figure.4 illustrates this. The curve in Fig.2, which we introduced above in this section, is one of the recorded light-intensity changes. From those intensity changes the time dependence of the averaged value for $[I_{max}(\mathbf{r}) - I_{min}(\mathbf{r})]\{i\delta_{kl}(\mathbf{r}) - (2/\pi)i\}$ (k = 0, l = 1,2,3,…) is calculated. As only the absolute value of the deformation phase is obtained, the direction of the object deformation cannot be determined. In other words, we do not know whether an optical path length increases or decreases. Therefore, in initial stage of the deformation measurement (the continuous capturing of specklegrams) we shorten the reference optical path length with a rate greater than the deformation speed. (In this experiment we pull the object along constant direction.) From the specklegrams captured during the shortening, the absolute deformation phase is calculated with the technique written above. The light-intensity changes at all the pixels during this shortening are related to the same direction in the phase change as that of only the shortening of the reference path length. Thus we can relate the phase change to the deformation direction correctly, which is positive under the shortening of the reference path length. Besides we can shorten the reference path length until the total phase changes during the shortening become greater than 2π on any pixel, so that we can obtain $I_{max}(\mathbf{r})$, $I_{min}(\mathbf{r})$ even at a nondeforming point.

In addition to $I_{max}(\mathbf{r})$ and $I_{min}(\mathbf{r})$ we already know $I(\mathbf{r},t_0)$ (t_0 is the time of the starting point of the capture process) and $I(\mathbf{r},t_j)$ (t_j is the time when the phase change due only to shortering becomes π/2 and the total phase change at t_j due to both shortening and deformation is bigger than 0 but less than π). From them $\cos[\theta(\mathbf{r},t_0)]$ and $\cos[\theta(\mathbf{r},t_j)]$ are easily calculated, and phase change $\Delta\theta(\mathbf{r}, t_j - t_0)$ $[= \theta(\mathbf{r}, t_j) - \theta(\mathbf{r}, t_0)]$ is correctly extracted. Regarding them, we can use the neat relations,

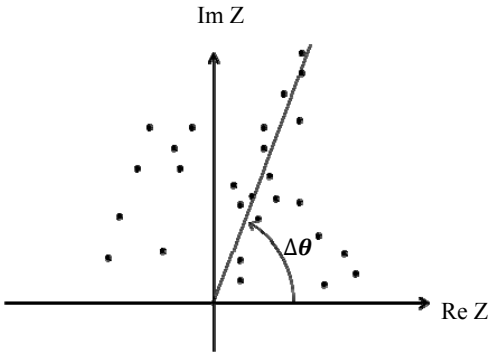

Fig. 4. Upper half complex plane plot of Z = $[I_{max}(\mathbf{r}) - I_{min}(\mathbf{r})]\exp[i\,\delta(\mathbf{r},t)]$. $\Delta\theta$ is the phase of the average value for $[I_{max}(\mathbf{r}) - I_{min}(\mathbf{r})]\{\exp[i\delta(\mathbf{r},t)] - (2/\pi)i\}$. The number of points is 50, and one point overlaps

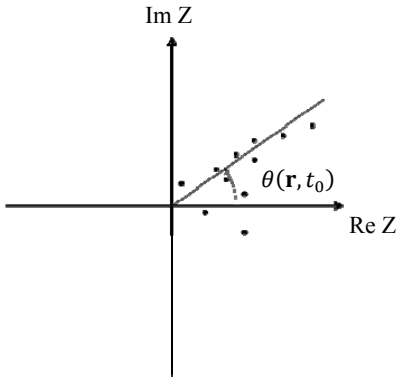

Fig. 5. Complex plane plotting of $\cos[\theta(\mathbf{r},t_0)]\sin[\Delta\theta(\mathbf{r},t_j - t_0)] + i\sin[\theta(\mathbf{r},t_0)]\sin[\Delta\theta(\mathbf{r},t_j - t_0)]$, where t_k is from t_j to t_j

$$\cos[\,\theta(\mathbf{r},t_0) + \Delta\theta(\mathbf{r},t_j - t_0)] = \cos[\theta(\mathbf{r},t_0)]\cos[\Delta\theta(\mathbf{r},t_j - t_0)] - \sin[\,\theta(\mathbf{r},t_0)]\sin[\Delta\theta(\mathbf{r},t_j - t_0)]. \quad (4)$$

From Eq. (4) we can calculate $\sin[\theta(\mathbf{r},t_0)]\sin[\Delta\theta(\mathbf{r},t_j - t_0)]$ with

$$\sin[\theta(\mathbf{r},t_0)]\sin[\Delta\theta(\mathbf{r},t_j - t_0)] = \cos[\theta(\mathbf{r},t_0)]\cos[\Delta\theta(\mathbf{r},t_j - t_0)] - \cos[\,\theta(\mathbf{r},t_0) + \Delta\theta(\mathbf{r},t_j - t_0)]. \quad (5)$$

From $\sin[\theta(\mathbf{r},t_0)]\sin[\Delta\theta(\mathbf{r},t_j - t_0)]$ given by Eq. (5) and $\cos[\theta(\mathbf{r},t_0)]\sin[\Delta\theta(\mathbf{r},t_j - t_0)]$ already obtained, we can extract phase $\theta(\mathbf{r},t_0)$ by

$$\theta(\mathbf{r},t_0) = \arg\{\cos[\theta(\mathbf{r},t_0)]\sin[\Delta\theta(\mathbf{r},t_j - t_0)] + i\sin[\theta(\mathbf{r},t_0)]\sin[\Delta\theta(\mathbf{r},t_j - t_0)]\}. \quad (6)$$

Note that a change in phase $\Delta\theta(\mathbf{r},t_j - t_0)$ is positive in shortening the reference path length. This phase can be extracted not only from the specklegram at t_j but also from all the specklegrams captured before t_j. Then $\cos[\theta(\mathbf{r},t_0)]\sin[\Delta\theta(\mathbf{r},t_k - t_0)] + i\sin[\theta(\mathbf{r},t_0)]\sin[\Delta\theta(\mathbf{r},t_k - t_0)]$ are calculated with k ($k < j$) and are plotted on the complex plane as shown in Fig. 5. By extracting the line intersecting the origin, O, and a gravity point of all the plotted points, $\theta(\mathbf{r},t_0)$ can be extracted precisely.

2.2. Speckle Phase after the Starting Point of the Measurement

We calculate the absolute value $|\theta(\mathbf{r},t)|$ of its speckle phase after the starting point in Eq. (2). Regarding the absolute value $|\theta(\mathbf{r},t)|$ we also consider both signed values, $-|\theta(\mathbf{r},t)|$ or $+|\theta(\mathbf{r},t)|$, and calculate the phase change $\delta'(\mathbf{r},t)$ from the starting point t_0 by

$$\delta'(\mathbf{r},t) = \pm|\theta(\mathbf{r},t)| - \theta(\mathbf{r},t_0). \quad (7)$$

where $\delta'(\mathbf{r},t)$ has a right phase change with 50% possibility. For every pixel position in the local area around $\mathbf{r}$, we plot the values given by $[I_{max}(\mathbf{r}) - I_{min}(\mathbf{r})]\exp[i\delta'(\mathbf{r},t)]$ on the complex plane. Fig. 6(a) shows the plotted points, and we can see that the distribution of the plotted points has no symmetry. By averaging all the plotted points, we obtain a real component $C_r(\mathbf{r},t)$ and an imaginary component $C_i(\mathbf{r},t)$ of the average value. Deformation phase $\Delta\theta'(\mathbf{r},t)$ after the starting point t_0 is then calculated as

$$\Delta\theta'(\mathbf{r},t) = \arg[C_r(\mathbf{r},t) + iC_i(\mathbf{r},t)]. \quad (8)$$

As described above, one of the two values $\delta'(\mathbf{r},t)$ in Eq. (7) is the right deformation phase, but the other is

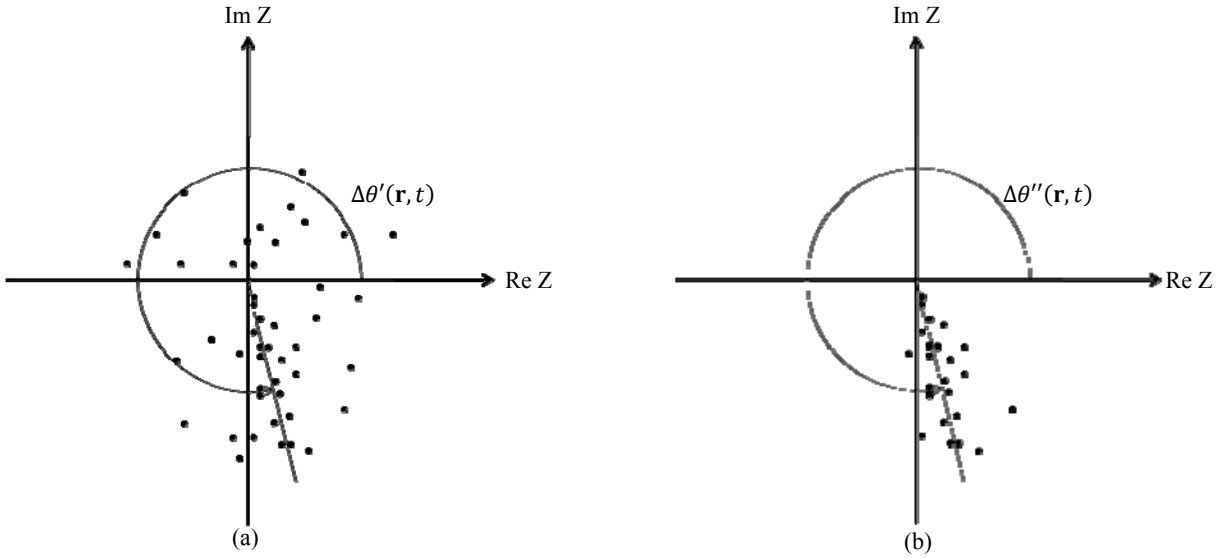

Fig. 6. (a) Complex plane plot of values calculated by $[\boldsymbol{I_{max}}(\mathbf{r}) - \boldsymbol{I_{min}}(\mathbf{r})]\exp[i\boldsymbol{\delta}'(\mathbf{r},\boldsymbol{t})]$. (b) Complex plane plot of the values that are selected from the points shown in Fig. 6(a).

affected by random speckle phase and is considered to be farther from $\Delta\theta'(\mathbf{r},t)$ than the former. Therefore, concerning the two values, we eliminate the one that is farther from $\Delta\theta'(\mathbf{r},t)$. Fig. 6(b) shows the remaining values. The remaining values are almost related to right deformation phase on the pixels in the local area, and $\Delta\theta''(\mathbf{r},t)$ given by averaging over them is considered to be a more accurate deformation phase. $\Delta\theta''(\mathbf{r},t)$ is the wrapped value from $-\pi$ to π. Then we calculate an unwrapped value $\Delta\theta'''(\mathbf{r},t)$ through temporally phase by unwrapping by

$$\Delta\theta'''(\mathbf{r},t_n) = \sum_{l=1}^{l=\mathrm{n}} \arg\{\exp i[\Delta\theta''(\mathbf{r},t_l) - \Delta\theta''(\mathbf{r},t_{l-1})]\}. \tag{9}$$

The deformation phase during a term from t_p to t_q is given by

$$\psi(\mathbf{r},t_q - t_p) = \Delta\theta'''(\mathbf{r},t_q) - \Delta\theta'''(\mathbf{r},t_p). \tag{10}$$

2.3. Speckle Phase in a large deformation

We could extract accurate deformation phase with the above technique. But the above technique could not extract the phase of a large deformation, because the large deformation changes a shape of speckle and the shape change causes the situation. There is not stable difference between $I_{max}(\mathbf{r})$ and $I_{min}(\mathbf{r})$ and phase changes rapidly. In other words, light-intensity seems to change irregularly as shown in Fig. 7. Thus if we carry on capturing specklegrams and try extracting deformation phase with the above technique about the large deformation, difference in the extracted phases in the local area gradually increase. The increasing difference interferes with extracting accurate deformation phases, and eventually extraction becomes impracticable. It is very fatal for deformation measurement in the large deformation.

We developed a method which can extract accurate deformation phase in a previous study. The method can extract phase accurately at any time. Then, let us consider a light-intensity change $I(\mathbf{r},t)$ contains the noise component of a light-intensity and the dc component given by

$$I(\mathbf{r},t) = A\cos\{\Theta + \emptyset(\mathbf{r},t)\} + Bn + C. \tag{11}$$

$$\Theta = \Delta\theta'''_{t_k} - \Delta\theta'''_{t}\,. \tag{12}$$

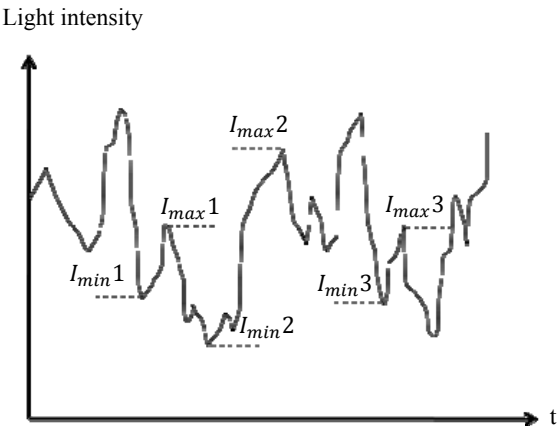

Fig. 7. Fluctuating modulation interferenced light intensity changes.

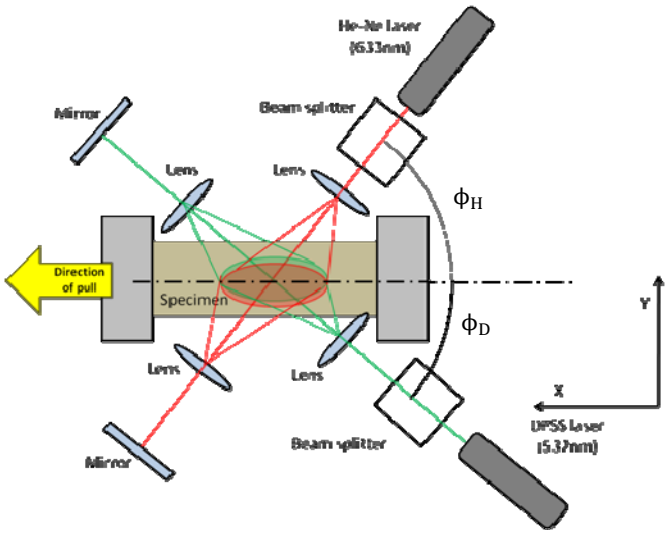

Fig. 8. The overhead view of the optical layout.

where A is the amplitude, $\emptyset(\mathbf{r},t)$ is the phase which we want to extract at time t, Θ is the deformation phase from time t_k to t, $\Delta\theta'''_{t_k}$ is the phase which is less 2π than the phase $\Delta\theta'''_{t}$, Bn is the noise component and C is the dc component. In order to extract the phase $\emptyset(\mathbf{r},t)$, we calculate $I_c(\mathbf{r},t)$ and $I_s(\mathbf{r},t)$ given by

$$I_c(\mathbf{r},t) = \int_{t_k}^{t} I(\mathbf{r},t_k - t_m)\cos\{\Theta(\mathbf{r},t_k - t_m)\}\frac{\mathrm{d}\Theta(\mathbf{r},t_k - t_m)}{\mathrm{d}t_m}\mathrm{d}t_m$$
$$= \int_{-2\pi}^{0} \mathrm{I}(\mathbf{r},\Theta)\cos\Theta\mathrm{d}\Theta = \int_{-2\pi}^{0}[\mathrm{A}\cos\{\Theta+\emptyset(\mathbf{r},t)\} + \mathrm{Bn} + \mathrm{C}]\cos\Theta\mathrm{d}\Theta \approx \mathrm{A}\pi\cos\emptyset\,. \quad (13)$$

$$I_s(\mathbf{r},t) = \int_{t_k}^{t} I(\mathbf{r},t_k - t_m)\sin\{\Theta(\mathbf{r},t_k - t_m)\}\frac{\mathrm{d}\Theta(\mathbf{r},t_k - t_m)}{\mathrm{d}t_m}\mathrm{d}t_m$$
$$= \int_{-2\pi}^{0} \mathrm{I}(\mathbf{r},\Theta)\sin\Theta\mathrm{d}\Theta = \int_{-2\pi}^{0}[\mathrm{A}\cos\{\Theta+\emptyset(\mathbf{r},t)\} + \mathrm{Bn} + \mathrm{C}]\sin\Theta\mathrm{d}\Theta \approx -\mathrm{A}\pi\sin\emptyset\,. \quad (14)$$

where because Bn and C do not intercorrelate with the deformation phase, we use the following equations.

$$\int_{-2\pi}^{0}(\mathrm{Bn}+\mathrm{C})\cos\Theta\mathrm{d}\Theta = 0. \quad (15)$$

$$\int_{-2\pi}^{0}(\mathrm{Bn}+\mathrm{C})\sin\Theta\mathrm{d}\Theta = 0. \quad (16)$$

From Eq. (13) and Eq. (14), we can get value of the phase $\emptyset(\mathbf{r},t)$ given by

$$\emptyset(\mathbf{r},t) = \arg\{I_c(\mathbf{r},t) - iI_s(\mathbf{r},t)\}. \quad (17)$$

We can cut off the signal that does not relate to the deformation by using Eq. (13) and (14) and calculate the right phase $\emptyset(\mathbf{r}, t)$ on every pixel from Eq. (17). We can reset the increasing difference in the deformation phases in the local area by substituting the right phase $\emptyset(\mathbf{r}, t)$ to the initial phase $\theta(\mathbf{r}, t_0)$ in Eq. (7), and the reset enables to extract accurate the deformation phase in the large deformation.

2.4. Deformation Measure along two directions

The side view of the optical layout of each laser is shown in Fig. 1. The overhead view of the optical layout of two direction measurement is shown in Fig. 8. The directions, which we want to measure, are the tension direction X and the direction Y normal to X. We have to calculate an amount of deformation along X and Y from deformation phase which are related to irradiation directions of laser. We can calculate the deformation d along irradiation directions of each laser by

$$\mathrm{d} = \psi \frac{\lambda}{4\pi \sin\alpha}. \tag{18}$$

where λ is wavelength of a laser and α is angle of incidence in Fig. 1. We can calculate deformation along X and Y by

$$\mathrm{d_x} = \mathrm{d_D} \cos\phi_\mathrm{D} + \mathrm{d_H} \cos\phi_\mathrm{H}. \tag{19}$$
$$\mathrm{d_y} = \mathrm{d_D} \sin\phi_\mathrm{D} - \mathrm{d_H} \sin\phi_\mathrm{H}. \tag{20}$$

where $\mathrm{d_x}$ is deformation along X, $\mathrm{d_y}$ is deformation along Y, $\mathrm{d_D}$ is deformation along irradiation direction of DPSS laser, $\mathrm{d_H}$ is deformation along irradiation direction of He-Ne laser, ϕ_D is the angle between X and irradiation direction of DPSS laser and ϕ_H is the angle between X and irradiation direction of He-Ne laser.($\phi_\mathrm{D} + \phi_\mathrm{H} = \pi/2$)

3. Experiment, Results and Discussion

3.1. Experiment

The optical layout used in this experiment is shown in Fig. 1 and Fig. 8. This layout was set up to confirm experimentally that the proposed technique can measure deformation along two directions correctly. In this experiment we used He-Ne laser whose wavelength is 632nm and DPSS laser whose wavelength is 532nm. The angle ϕ_H was about 51 degrees, and the angle ϕ_D was about 39 degrees. Each beams of laser was divided by beam splitter. The divided beams illuminated a diffuse surface along the right oblique angle and the left oblique angle respectively. Both of the right angle and the left angle were set up to be equal in this experiment. The angle for He-Ne laser was 58 degrees and the angle for DPSS laser was 63 degrees. The diffuse object was an aluminum plate which was sprayed with white paint and had 0.5mm thickness and 7mm gauge width, 35mm gauge length. To ensure the breaking position, we scratched the underside of the plate on central portion of its gauge. The aluminum plate was pulled by the tensile testing machine with a tension speed of about 1micro-meter/sec. The color camera was a CCD camera (Basler scA1390-17gc), which can capture with the rate of about 60frames/sec, and was equipped with fixed focal length lens (Nikkor 50mm). Specklegrams with 400×50 pixels were captured until the aluminum plate was broken.

3.2. Results and Discussion

We show experiment results of deformation along two directions of an aluminum plate. The broken aluminum plate after the measurement is shown in Fig. 9. This shows the measurement area enclosed with a solid line and the break happened at center of measurement area. In order to capture high-resolution specklegrams under deforming, we scratched the underside of the plate. The extracted deformation phases in early deformation are shown in Fig. 10(a) and 10(b). The whiter it is, the larger the amount of the deformation phase, and the blacker it

is, the smaller the amount is. From those extracted phases, deformation d_x and d_y are calculated by Eq. (19) and Eq. (20) and are shown in Fig. 11(a) and 11(b). From Fig. 11(a), we see that the amount of the deformation along X is linearly larger in proportion to going left side. From Fig. 11(b), we also see that the amount of the deformation along Y on upside area is less and on downside area is more. Those results mean that the deformation along X has uniform strain and the deformation along Y is small constricted. To make those results clearly, each amount of the deformation was divided by 5 micro-meters and 2 micro-meters, and their remainders are shown in Figure 12(a) and 12(b). The shorter a period of the remainder is, the larger deformation is. Comparing remainders enable us to understand how large deformation is. From Fig. 12 we see that the period is almost constant, thus, and understand that deformation is homogeneous in the early deformation.

The extracted phases in just before break are shown in Fig. 13(a) and 13(b). From those extracted phases we calculated deformation along two directions and show the results in Fig. 14(a) and 14(b). Fig. 15(a) and 15(b) each shows a remainder of the deformation divided by 5 micro-meters and 2 micro-meters. From Fig. 15 we see that both of deformations at breaking position are larger than in the other place because both of the periods in breaking place are shorter than in the other.

The measured results show that the proposed method can measure correctly deformation along two directions because the results satisfy the phenomenons of the tensile deformation. All the images shown from Fig. 10 to Fig. 15 can be displayed with animation data, which show deformation intensity dependence on time.

4. Conclusion

We proposed the new method which can measure deformation along two directions with two lasers and one color camera. To verify the validity of the method, we carried out deformation measurement of the aluminum plate. Experimental results are described in the above section. They confirmed that the method can measure deformation along two directions correctly.

In addition, the proposed technique has potential to measure deformation along three directions, two in-planes and one out-of-plane, by appending one more laser to the optical system.

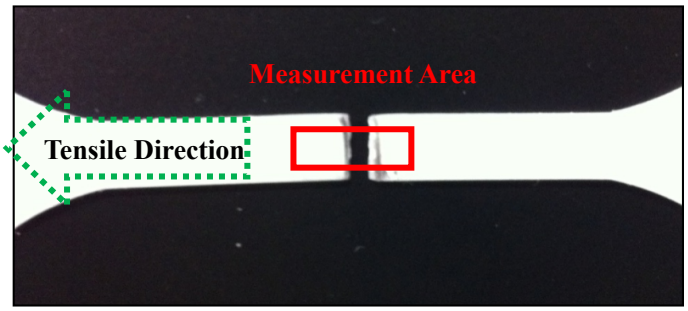

Fig. 9. Broken aluminum plate.

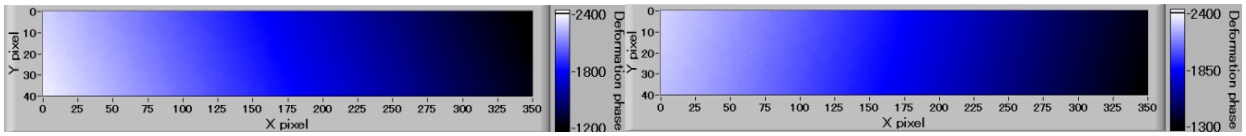

(a) (b)

Fig.10. Extracted phases in the early deformation, (a) extracted phase with DPSS laser(wavelength 532nm). (b) extracted phase with He-Ne laser(wavelength 632nm).

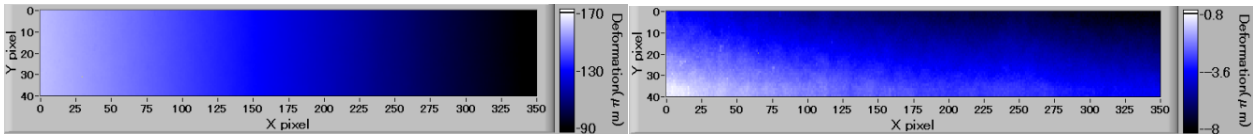

(a) (b)

Fig. 11. Deformation in the early deformation, (a) deformation along X. (b) deformation along Y.

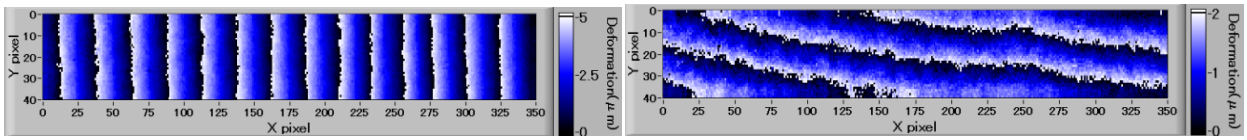

(a) (b)

Fig. 12. A remainder of an amount of deformation in early deformation, (a) deformation along X divided by 5 micro-meters. (b) deformation along Y divided by 2 micro-meters.

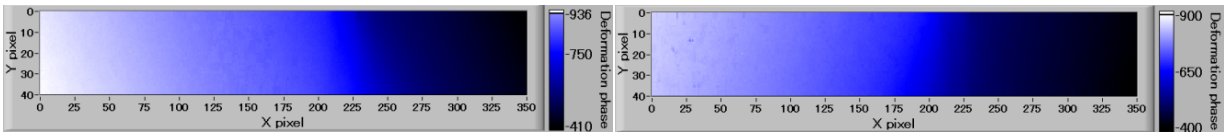

(a) (b)

Fig. 13. Extracted phases in just before break, (a) extracted phase with DPSS laser(wavelength 532nm). (b) extracted phase with He-Ne laser(wavelength 632nm).

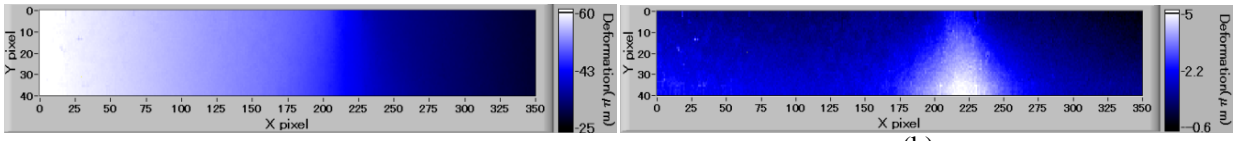

(a) (b)

Fig. 14. Deformation in just before break, , (a) deformation along X. (b) deformation along Y.

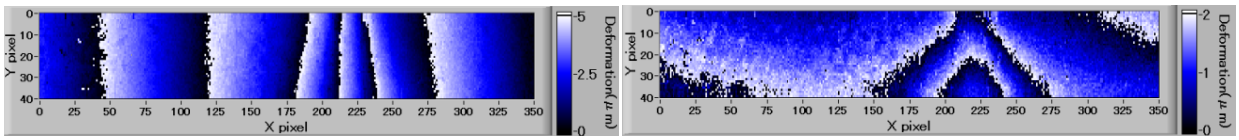

(a) (b)

Fig. 15. A remainder of an amount of deformation in just before break, (a) deformation along X divided by 5 micro-meters. (b) deformation along Y divided by 2 micro-meters.

5. References

1) K. Ceath, “Phase-shifting speckle interferometry,” Appl. Opt.24, 3053-3058 (1985).
2) A. J. P. Haasteven and H. J. Frankena, “Real-time displacement measurement using a multicamera phase-stepping speckle interferometry,” Appl. Opt. 33, 4137-4142 (1994).
3) E. Vikhagen, “Nondestructive testing by use of TV holography and deformation phase gradient calculation,” Appl. Opt. 29, 137-144 (1990).
4) J. Wang and I. Grant, “Electronic speckle interferometry, phase-mapping, and nondestructive testing techniques applied to real-time, thermal loading,” Appl. Opt. 34, 3620-3627 (1995).
5) A. Davila, D. Kerr, and G. H. Kaufmann, “Fast electro-optical system for pulsed ESPI carrier fringe generation,” Opt. Commun. 123, 457-464 (1996).
6) G. Pedrini and H. J. Tiziani, “Double-pulse electronic speckle interferometry for vibration analysis,” Appl. Opt. 33, 7857-7863 (1994)
7) M. Takeda, H. Ina, and S. Kobayashi, “Fourier-transform method of fringe-pattern analysis for computer-based topography and interferometry,” J. Opt. Soc. Am. 72, 156-160 (1982).
8) M. Adachi, Y. Ueyama, and K. Inabe, “Automatic deformation analysis in ESPI using one speckle interferometry of a deformed object,” Opt. Rev. 4, 429-432 (1997).
9) T. E. Carlsson and A. Wei, “Phase evaluation of speckle patterns during continuous deformation by use of phase –shifting speckle interferometry,” Appl. Opt. 39, 2628-2637 (2000).
10) M. Adachi, J. N. Petzing, and D. Kerr, “Deformation-phase measurement of diffuse objects that have started nonrepeatable dynamic deformation,” Appl Opt. 40, 6187-6192 (2001)
11) M. Adachi, M. Takayama, K. Inebe, and T. Matsumoto, “Mesurement of Large Changing Deformation Phase under Fluctuational Modulation of Speckle-Light Intensity Changes,” JSPE. 68, 1326-1330 (2002)